International Journal of
INTELLIGENT SYSTEMS AND APPLICATIONS IN ENGINEERING
ISSN:2147-6799 www.ijisae.org Original Research Paper

A Hybridized Particle Swarm – Grey Wolf Optimization (PS-GWO) Mechanism for the Design of OFDM-LFM Signals in MIMO Systems

S. V. Bharath Kumar Reddy* **and Ch. Sumanth Kumar**

Submitted: 17/09/2023 **Revised**: 18/11/2023 **Accepted**: 30/11/2023

Abstract: The Orthogonal Frequency Division Multiplexing (OFDM) linear frequency modulation (LFM) waveform has become the focus of much research due to its possible usage in Multiple-Input, Multiple-Output (MIMO) radar; nonetheless, its efficient design remains a hurdle. The OFDM-LFM signals are utilized to extensively examine the pulse compression feature of dynamically generated signals. In the most recent research, several coupled optimization methodologies have been developed to improve radar communication systems' overall efficiency. However, it comes with shortcomings such as calculations that are hard to understand, a substantial miss rate, and decreased efficacy. To enhance the pulse compression qualities and suppress grating sidelobes, the suggested study aims to develop a hybrid Particle Swarm integrated Grey Wolf Optimization (PS-GWO) mechanism for generating OFDM-LFM signals with suppressed grating side lobes. In this case, the intended LFM waveform is modified to enhance its periodic frequency steps whilst retaining orthogonal and sidelobe properties that are symmetrical. Through simulation research, the performance and results of the proposed PS-GWO based joint optimization model have been evaluated and compared using various pulses compression features. When compared to the most recent methods already in use, the findings of the investigation demonstrate that the suggested optimization model provides more effective results.

Keywords: *Multiple inputs and outputs (MIMO), Radar Communication, Spatial Synthesis Signals, Orthogonal Frequency Division Multiplexing (OFDM), Particle Swarm Integrated Grey Wolf Optimization (PS-GWO), and Linear Frequency Modulation (LFM).*

1. Introduction

Multiple inputs and outputs (MIMO) radar employs a wide range of waveforms for transmission and has the ability to receive signals that have been collaboratively processed by a variety of receiving antennas [1-3]. It makes use of widely spread transmitters and receivers to simultaneously view the target from a number of distinct angles, creating spatial variety that can improve radar detection effectiveness. In order to improve the MIMO radar [4] technique's performance when generating waveforms, orthogonal properties that can reduce evaluation factors can be enhanced with low interference and high resolution, increased detection capabilities. Recently, many application systems [5-7], including target detection, jamming recognition, and radar imaging applications, use Linear Frequency Modulated (LFM) signals. The ability to transmit a long-duration, low-peak-power pulse [6, 8, 9] and then compress it into a considerably shorter, compressed pulse with a significantly greater peak output makes pulse compression essential to radar signal processing. Additionally, it is crucial in scenarios where a radar system's ability to transmit high peak power is either difficult or unfeasible, such as in millimeter-wavelength radar, space-borne radar, and phased array radar that uses semiconductor devices. Both the signal-to-noise ratio (SNR) [10-12] of the return signal and the range resolution of radar can be enhanced via pulse compression. As a result, pulse compression is a fundamental building block for contemporary radar applications like target detection, navigation, radar system imaging, and many others. In the past, pulse compression has been accomplished by utilizing the well-known matched filter approach, which may be utilized to increase the output SNR of the radar signal in a white Harmonic noise environment. However, the matching filtering will also produce adversely high lower order harmonics [13, 14]. As a result, whenever a weak scatter falls in an area with high sidelobes of a strong scatter, it may be covered, which has an adverse effect on the effectiveness of target recognition and monitoring. Fig 1 (a) shows the general block representation of the MIMO radar communication system, and the graphical representation of the proposed framework is shown in Fig 1 (b).

Department of Electrical, Electronics and Communication Engineering, GITAM School of Technology, Visakhapatnam, India.
**Corresponding Author's Email: sbharath@gitam.edu*
Corresponding author

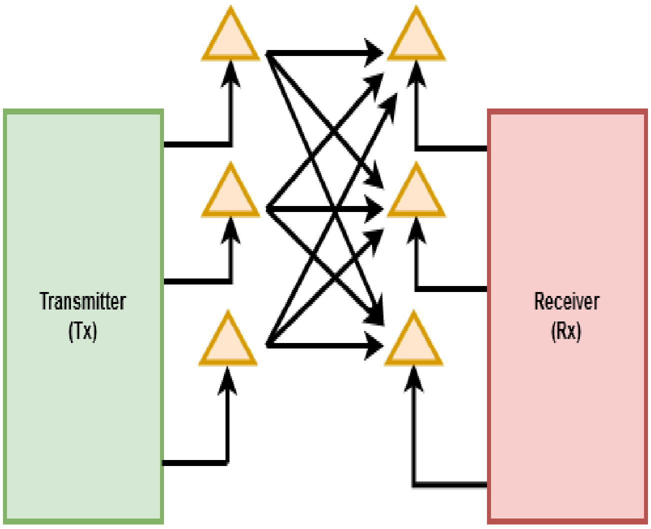

Fig 1 (a). MIMO communication system

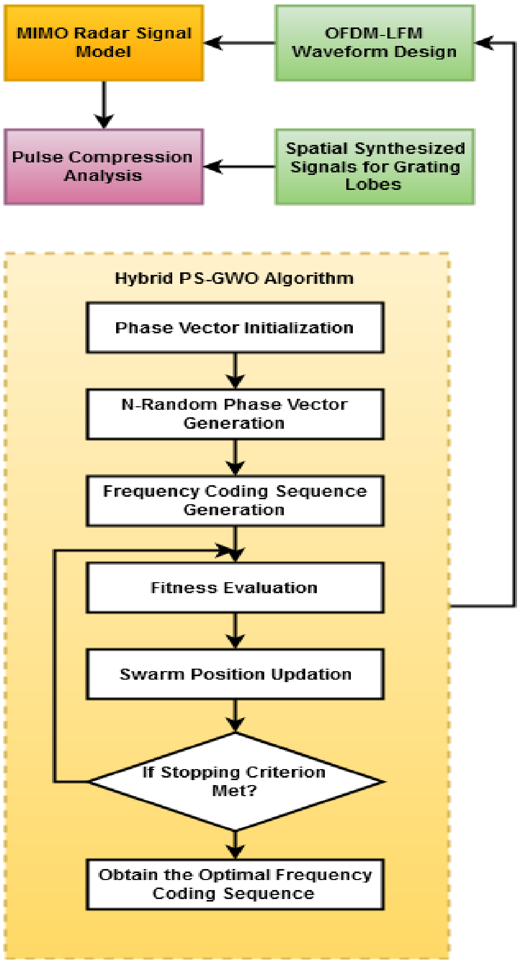

(b)

Fig 1 (a) MIMO communication system (b) Graphical representation of the proposed model.

In order to improve the design of OFDM-LFM waveforms with higher pulse compression property, the proposed work aims to create a new joint optimization model [25, 26]. Additionally, the suggested system aims to achieve orthogonality, a constant envelope, and a lower sidelobe level. The key contributions of this paper are as follows:

- The suggested framework efficiently uses Linear Frequency Modulated (LFM) signal to improve the performance of radar communication.
- A hybrid and novel Particle Swarm Optimization integrated with Grey Wolf optimization mechanism, named as PS-GWO is used to generate an optimal OFDM-LFM signal.
- Using joint optimization, the PSO integrated Sequential Quadratic Programming (SQP) technique is used to effectively eliminate the side lobes.
- An extensive simulation is conducted with different parameters in order to verify the effectiveness and feasibility of the proposed communication model.

The remaining portions of this article are split into the following categories: In Section 2, various optimization approaches are examined in order to enable effective radar communication in MIMO-OFDM systems. Section 3 presents a comprehensive overview of the PS-GWO based communication system. In Section 4, the simulation and comparison findings of the proposed hybrid optimization based communication mechanisms are validated using different parameters. In Section 5, the overall paper is summarized together with its future scope.

2. Related Works

This section examines a few of the traditional optimization methods that are employed in MIMO-OFDM communication systems to ensure a successful radar transmission. Additionally, it examines each mechanism's benefits and drawbacks in light of its distinguishing characteristics and primary purposes.

Li, et al [27] designed a multi-carrier phase code signal for solving the problem of radar anti-jamming problem. Here, the authors mainly focused on improving the communication efficiency of the radar system with reduced interferences. *Huang, et al* [28] introduced a joint optimization model by incorporating the functions of Semi Definite Relaxation (SDR) for minimizing the output signal interference of the radar system. For validating this system, the different types of characteristics such as beam pattern, signal to noise ratio, computational complexity, and waveform properties. Here, the transmit waveform was optimized for minimizing the signal interference without distortions. Moreover, the constrained waveform was designed with constant envelope and energy characteristics. *Zhao, et al* [29] deployed a Non-continuous Piecewise Non-Linear Frequency Modulation (N-PNLFM) waveforms in the radar systems. Here, the signal optimization was performed by using an efficient PSO technique. Also, this paper objects to minimize the repetitive sidelobes by using the optimization model. The benefits of this work were increased efficiency, optimized performance, and error rate. *Xenaki, et al* [30] implemented a distributed optimization methodology for enhancing the spatial sampling of MIMO systems. The purpose of this work was to utilize the SAS geometry in a strip map mode for optimizing the reflectivity function. *Li, et al* [20] suggested a Riemannian Geometric optimization methodology for maximizing the output signal ratio with improved target detection performance. The purpose of this work was to implement the manifold optimization mechanism for enabling an efficient data transmission in radar system with reduced iteration complexity. The advantages of this work were increased efficiency, detection performance and easy to understand. *Qian, et al* [31] constructed a constrained maximization problem for improving MIMO radar communication. Here, the performance and efficacy of the suggested model has been validated in terms of SINR and cross ambiguity functions. The key merit of this work was, it attained a reduced channel estimation error with ensured robustness. *Wang, et al* [32] deployed a sparse array optimization technique for embedding the communication information with the MIMO radar. The unique phases induced by antenna displacements in a sensor array enable array configuration for symbol embedding. A hybrid selection and permutation technique is used in this case to perform waveform-antenna paring with array reconfiguration for communication symbol embedding in MIMO radars, which can result in a high data rate and much lower symbol error rate.

Rihan, et al [33] suggested an interference alignment approach for an enabling an effective spectrum sharing in radar and communication systems. Here, an iterative algorithm has been deployed to improve the SINR of the radar system. By alternately optimizing the two sub-algorithms, the main iterative algorithm is suggested to jointly optimize transmit and receive beam forming filters of both systems. Here, the central control unit (CCU), the foundation of such architecture, may be functionally connected with the radar control center, which is typically equipped with remarkable computational power, to carry out complex processing tasks. The primary advantage of this work was, it has a better convergence speed for strong and weak interference channels. However, high computational complexity and processing time are the major problems of this work. *Shi, et al* [34] introduced a new pulse compression method, named as, Offset Quadrature Amplitude Modulation (OQAM) based OFDM system for MIMO communication.

3. Proposed Methodology

This section provides the complete explanation for the proposed hybrid PS-GWO based MIMO communication system with its overall work flow and clear explanations. This work's key contribution is the creation of an effective joint optimization method that combines the capabilities of hybrid PS-GWO and Sequential Quadratic Programming (SQP) mechanisms to create the best possible OFDM-LFM waveforms. Additionally, it intends to determine the frequency codes and phases for optimal orthogonal sidelobe suppression for high grating sidelobes.

3.1. OFDM-LFM based Radar Signal Model

To reduce the peak power of radar, pulse compression is one of the widely utilized mechanisms in communication systems. Because the longer pulse is used at the transmitter side during regulating operations, it enables the proper usage of long pulses. The OFDM coded waveform can be sent by the transmit antennas in MIMO systems using a variety of carrier frequencies. The primary purpose of the OFDM-LFM waveforms is to exchange fixed frequency signals. The sample LFM signals from the two separate LFM models that were produced using the matched filtering technique are shown in Fig. 2. In most cases, the LFM signals are made up of inphase and quadrature band signals, which are totally dependent on the chirp signal's scientific conditions. It is also known as the frequency balanced waveform, where the carrier frequency can change over a specific time period.

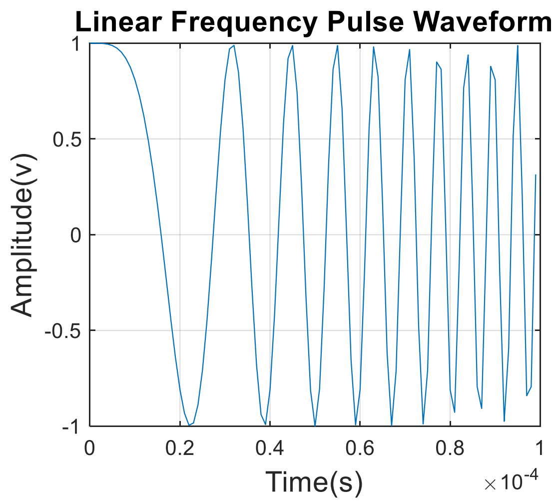

(a)

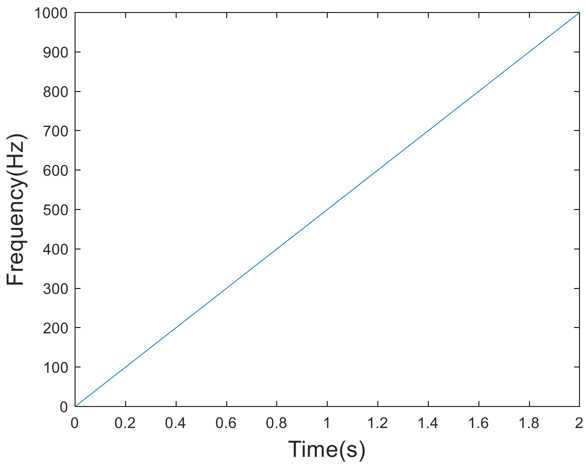

(b)

Fig. 2. Sample LFM signals (a) and (b)

By utilizing these waveforms, the energy in this model is evenly distributed over the frequency ranges. Then, the expression is mathematically written as follows:

$$w_a(t) = r(t)e^{j2\pi(f_c t + (1/2)\mu t^2)} \quad (1)$$

$$r(t) = \begin{cases} 1, & -\frac{T}{2} \leq t \leq T/2 \\ 0, & Else \end{cases} \quad (2)$$

$$\mu = MB_w/T \quad (3)$$

$$f_c = f_p + c_a \Delta f \quad (4)$$

Where, $w(t)$ indicates the OFDM-LFM waveform, $r(t)$ is the rectangular window, T denotes the time period, $a = 1,2, \dots A$, μ represents the chirp rate, MB_w defines the modulated bandwidth, f_c is the carrier frequency, f_p indicates the centre frequency, c_a is the code of frequency, and Δf is the frequency step. According to the signal processing structure of radar communication system, the receiver beamformer by the space time matched filtering technique are as follows:

$$f(\theta, \theta_h, \tau) = \int_{-\infty}^{\infty} y(\theta, t) y^*(\theta_h, t - \tau)\, dt \quad (5)$$

Where, τ indicates the delay time, and θ_h is the direction of beam. If $\theta_h = \theta$, the pulse compression rate is obtained that is corresponding to the autocorrelation model of spatial synthesis signal. Else, the cross correlation function is obtained that lies in two different locations. By using the function $f(\theta, \theta_h, \tau)$, the process of target detection is enhanced for instance, the autocorrelation sidelobes may leads false detection, which creates the interference among various targets.

The best way to analyze and optimize the autocorrelation function is the tuning of compression property for target detection as mentioned in equ (5).

3.2. Pulse Compression Analysis

A type of spread-spectrum technology called OFDM uses a single communication path to transmit the carriers. Likewise, each sub carrier might carry a tiny portion of the overall signal.

Typically, the modulation strategy with the chosen number of bits, such as Binary Phase Shift Keying (BPSK), Quadrature Phase Shift Keying (QPSK), and Quadrature Amplitude Modulation (QAM) is used to form the OFDM signals. The fundamental block representation of OFDM system is shown in Fig 3.

Based on the signal model, the results of pulse compression of the spatial synthesized signal are analyzed, and the results are given in below:

$$f(\theta, \tau) = \sum_{m=1}^{M} e^{j2\pi f_m \tau} \zeta_0(\tau) + \sum_{v=1}^{M-1} R_v(\tau) + \sum_{n=1}^{M-1} Z_n(\tau) \quad (6)$$

where,

$$\zeta_u(\tau) = \int_{-\infty}^{\infty} r(t) r(t-\tau) e^{j\pi|\mu t^2 - \mu(t-\tau)^2|} e^{j2\pi u t}\, dt \quad (7)$$

$$R_v(\tau) = \sum_{a=v+1}^{A} e^{j2\pi f_{c-v}\tau} e^{\frac{j2\pi v d \sin(\theta)}{\lambda}} \zeta_{f_c - f_{c-v}}(\tau) \quad (8)$$

$$Z_n(\tau) = \sum_{a=1}^{A-n} e^{j2\pi f_{c+n}\tau} e^{\frac{-j2\pi n d \sin(\theta)}{\lambda}} \zeta_{f_c - f_{c+n}}(\tau) \quad (9)$$

The equ (5) represents the main lobe, while the last two terms portray the left and right side lobes respectively. Then, the frequency code c_a is set as $a - (A+1)/2$, hence the carrier frequency at a^{th} position is represented as $f_c = c_a \Delta f$. Based on these models, it is analyzed that the same frequency step and modulation bandwidth can create the grating sidelobes at disparate positions.

3.3. Particle Swarm Optimization (PSO)

Generally, the PSO [35] is a population based meta-heuristic that produce more suitable solutions in a respectably practical amount of time and prevents a solution from being trapped to a local optimum. It is a well-known technique for resolving various engineering optimization issues. Moreover, a particle is defined as a hypothetical resolution, where the value of each particle's fitness is provided by the objective function. Also, the initialization of the particles is random, and each particle goes randomly through a multidimensional search space in search of a higher fitness value. Based on data from the particle's personal/local best position and global best position, its position is updated. Each iteration involves repeating this process, and the updated velocity is aided by inertia weights. Furthermore, the particle is subject to boundary limitations to ensure that the particle solution stays within the permitted range. PSO was initially thought of as a mathematical approach to handle optimization issues with optimized variables. Any values that provide the absolute answers without exhibiting any limits can be used for these optimized variables. In PSO, every possible solution is denoted as a particle with '*x*' position vector, '*w*' represented as a phase weighting factor and velocity is represented as '*v*'. The steps involved in the PSO mechanism are illustrated in below:

Step 1: Initialization of particles;

Step 2: *N* set of phase vectors are generated with the length of PTS sub-blocks (i.e. the swarm population size is represented as *N*).

Step 3: Then, the velocity *vi* is initialized as zero, and the size of both velocity and position components are same;

Step 4: Consequently, the particle fitness is estimated, and each particle's *l* best is fixed, where the estimated objective value is same as its current location. Then, *gbest* is fixed as the best position;

Step 5: All particles are updated throughout the iterations based on the following models:

$$vel_i(\tau+1) = w * vel_i(\tau) + r_1 * c1 * \left(pos^{lb}(t) - pos_i(t)\right) + r_2 * c2 * \left(pos^{gb}(\tau) - pos_i(\tau)\right) \quad (10)$$

$$pos_i(\tau+1) = pos_i(\tau) + vel_i(\tau+1) \quad (11)$$

Where, r1 and r2 are random values and c1 and c2 are local and global learning coefficients.

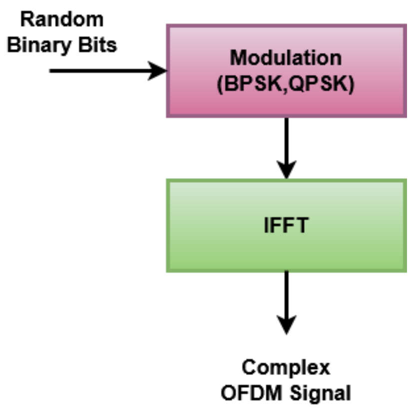

Fig.3. Structure of OFDM

3.4. Grey Wolf Optimization (GWO)

In nature, grey wolves have a leadership structure and a hunting system. The Grey Wolf Optimizer (GWO) algorithm imitates these features. For the purpose of mimicking the leadership hierarchy, four different varieties of grey wolves, including alpha, beta, delta, and omega, are used. The goal of the grey wolf optimization algorithm is to imitate the wolf leadership hierarchy and predatory behavior while using the grey wolf abilities of search, encirclement, hunting, and other predation-related tasks. The administration order and pursuit mechanism of wolves are copied by the GWO computation. To simulate the authority chain of command, four separate grey wolves - alpha, beta, delta, and omega must be taken into account. Hunting involves three crucial steps: looking for prey, surrounding prey, and attacking the prey. The three of these are used to carry out optimization techniques, which are denoted as $P(\alpha), P(\beta) and\ P(\delta)$. The velocities are determined by using the following equations:

$$V_\alpha = |C.P_\alpha(t) - P_i(t)| \quad (12)$$

$$V_\beta = |C.P_\beta(t) - P_i(t)| \quad (13)$$

$$V_\delta = |C.P_\delta(t) - P_i(t)| \quad (14)$$

Then, the positions are updated by using the following models:

$$P_1 = P_\alpha + B.V_\alpha \quad (15)$$

$$P_2 = P_\beta + B.V_\beta \quad (16)$$

$$P_3 = P_\delta + B.V_\delta \quad (17)$$

Where, B and C are the vector coefficients which are calculated by using the following models:

$$B = 2b.r_1 - b \quad (18)$$

$$C = 2.r_2 \quad (19)$$

$$P_{i+1} = \frac{P_1 + P_2 + P_3}{3} \quad (20)$$

The hybridization is performed based on the following models:

$$V_\alpha = w * vel_i(\tau) + r_1 * c1 * \left(pos^{lb1}(t) - pos_i(t)\right) + r_2 * c2 * \left(pos^{gb}(\tau) - pos_i(\tau)\right) \quad (21)$$

$$V_\beta = w * vel_i(\tau) + r_1 * c1 * \left(pos^{lb2}(t) - pos_i(t)\right) + r_2 * c2 * \left(pos^{gb}(\tau) - pos_i(\tau)\right) \quad (22)$$

$$V_\delta = w * vel_i(\tau) + r_1 * c1 * \left(pos^{lb3}(t) - pos_i(t)\right) + r_2 * c2 * \left(pos^{gb}(\tau) - pos_i(\tau)\right) \quad (23)$$

Consequently, the position updation is performed by using the following models:

$$P_1 = pos^{lb1} + B.V_\alpha \quad (24)$$

$$P_2 = pos^{lb2} + B.V_\beta \quad (25)$$

$$P_3 = pos^{lb3} + B.V_\delta \quad (26)$$

Where, B and C are the vector coefficients estimated by using the following models:

$$B = 2b.r_1 - b \quad (27)$$

$$C = 2.r_2 \quad (28)$$

$$P_{i+1} = \frac{P_1+P_2+P_3}{3} \quad (29)$$

$$E = \max_{\substack{p=1,2,\dots,P \\ 0<\tau\le T}} \left|f(\theta_p, \tau)\right| \quad (30)$$

3.5. Particle Swarm integrated Grey Wolf Optimization (PS-GWO)

In this work, the PS-GWO technique is mainly used to select the frequency steps based on the process of optimization. This approach enhances the strength of both types by improving the exploitation in particle swarm optimization and the exploration in the grey wolf optimizer. On the basis of this, this work introduces the PS-GWO algorithm, which combines the grey wolf and particle swarm optimization techniques. There are three primary concepts for improvement in this algorithm. First, it uses Tent mapping to initialize the population. Next, it uses a nonlinear control parameter strategy to coordinate the ability to explore and exploit. Finally, it is inspired by the PSO algorithm and uses a new position update equation of individuals that incorporates the knowledge of each individual's historical best solution to hasten convergence. Here, the joint optimization model based on a hybrid PS-GWO mechanism is implemented to design an OFDM-LFM waveforms. In which, the PS-GWO technique is used to perform optimization, and the SQP model is utilized to select the phases. Here, the different types of frequency codes are considered, where the PS-GWO is used to attain the better quality of design. By using a hybrid optimization techniques, two variables are perfectly optimized in a successive way. The PS-GWO based algorithm is given as:

PS-GWO Algorithm

Step 1: Phase vector initialization;

Step 2: Generate *N* random phase vectors in between 0 to 2 π as the elements of φ^0 and treat φ^0 as present phase vector;

Step 3: Initialize the frequency coding sequence and generate $\mathcal{F}^0$ different frequency coding sequences through stochastic permutations as the initial χ^0 number of swarms;

Step 4: With fixed phase vector φ^0 evaluate the fitness value using the cost function of each swarm in χ^0 according to cost function equation (24). Select $\mathcal{F}$ best swarms and form χ new current number of swarms;

Step 5: Sort the $\mathcal{F}$ swarms according to their fitness values and then apply SQP to the Q individuals. If the finer phase vectors φ_b exists then update $\varphi^0 = \varphi_b$. Like this select top 3 swarms α, β and δ;

Step 6: After selecting best three swarms update the position of each swarms ($\mathcal{F}^0$ *frequency coding sequence*) using the equations from (15) to (23) by comparing each swarm with best three;

Step 7: After updating the positions of all coding sequences and phase vectors in the present iteration calculate the fitness function for newly updated positions of all swarms. And go to step 5 and repeat the process till step 7 for all iterations;

Step 8: Find the optimal frequency coding sequence is the best swarm in all swarms and the resultant phase vector is the current phase vector φ^0;

4. Results and Discussion

This section compares and validates the simulation results of the suggested radar communication approach using a variety of evaluation metrics. Additionally, certain design examples are used to illustrate how effective and efficient the proposed PS-GWO performs the joint optimization process. This method was designed primarily for frequency code and phase optimization to reduce high grating sidelobes, with a focus on pulse compression to enhance reliable transmission.

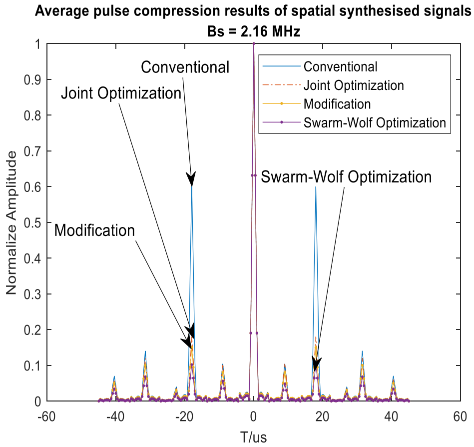

(a)

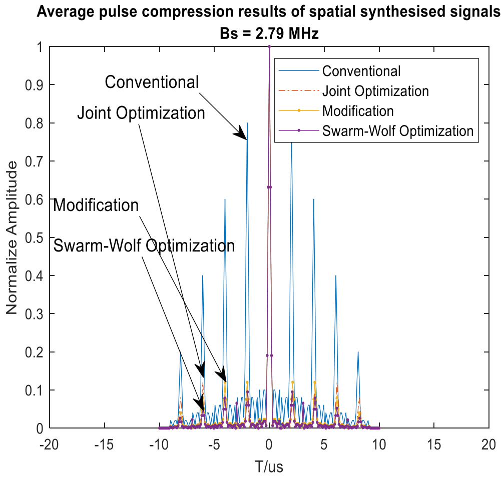

(b)

Fig. 4. Average pulse compression results (a) Bs = 2.16MHz and (b) Bs = 2.79MHz

Here, a modified optimization approach is used to reduce the sidelobes of the grating. The initial population, the number of particles for phase optimization, and the best global function are the general parameters taken into account by the PSO process. Two LFM waveforms are created here for comparison, with Bs = 2.16 MHz and 2.79 MHz, respectively. For the proposed PS-GWO based joint optimization technique, the average sidelobes of the waveforms are first calculated as shown in Fig 4.

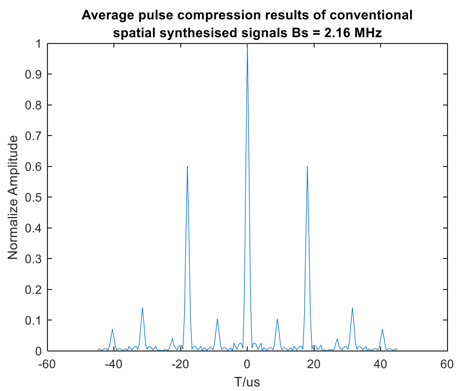

(a)

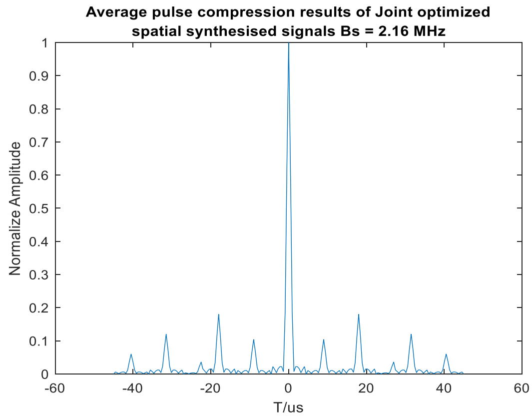

(b)

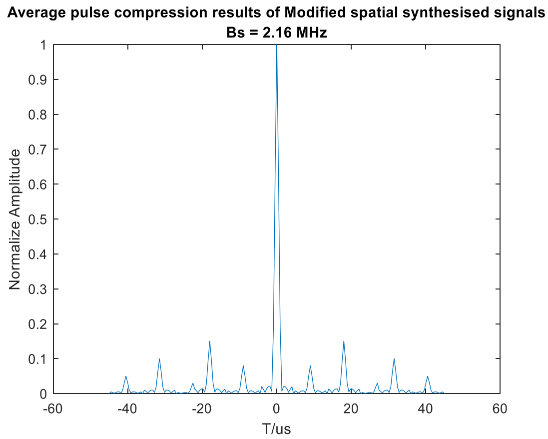

(c)

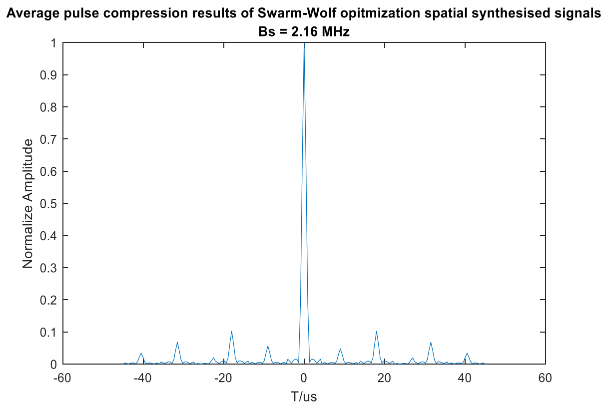

(d)

Fig. 5. Average pulse compression analysis Bs = 2.16MHz (a) Conventional spatial synthesized signals (b). Joint optimization based spatial synthesized signals (c). Modified spatial synthesized signals, and (d). PS-GWO based spatial synthesized signals.

In this case, the number of grating sidelobes produced by the traditional optimization processes may occasionally exceed that of the suggested model. Small peaks in the waveforms might occur as a result of the suggested model's incorporation of sink-like functions.

Furthermore, the PS-GWO model is used in the suggested model to synthesize the erroneous detection's waveforms, which are primarily generated by the grating sidelobes. In this investigation, the target detection performance of the optimization model is primarily estimated from the pulse compression features of the spatial synthesis signals. Additionally, the target detection performance at various targets is estimated using the spatial cross correlation functions.

In order to prove the effectiveness of the proposed PS-GWO mechanism, the pulse compression properties of the existing (i.e. convention, joint optimization, modified synthesized), and proposed PS-GWO techniques are separately validated and compared with Bs = 2.16GHz and Bs = 2.79GHz in Fig 5 and Fig 6 respectively.

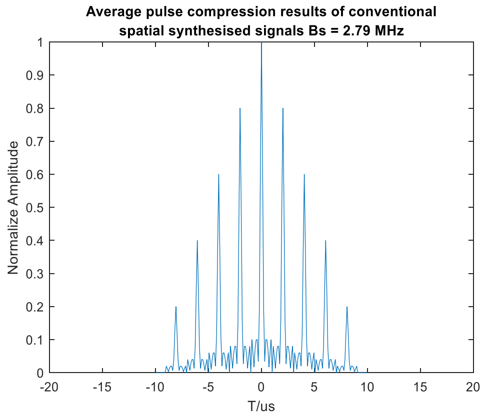

(a)

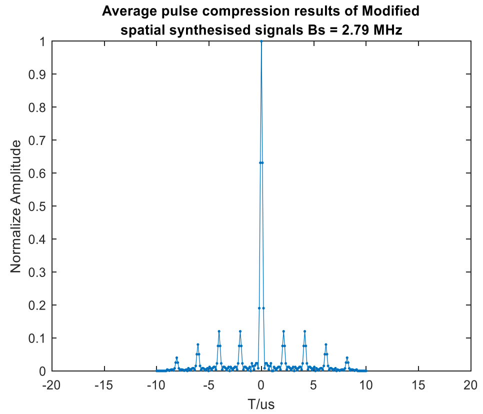

(b)

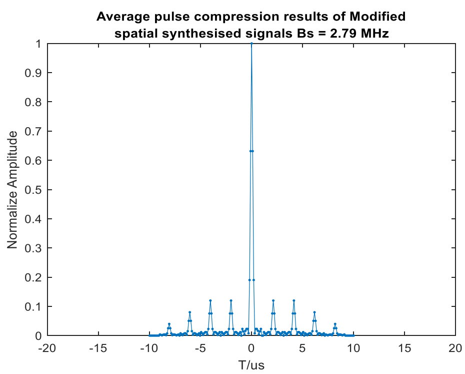

(c)

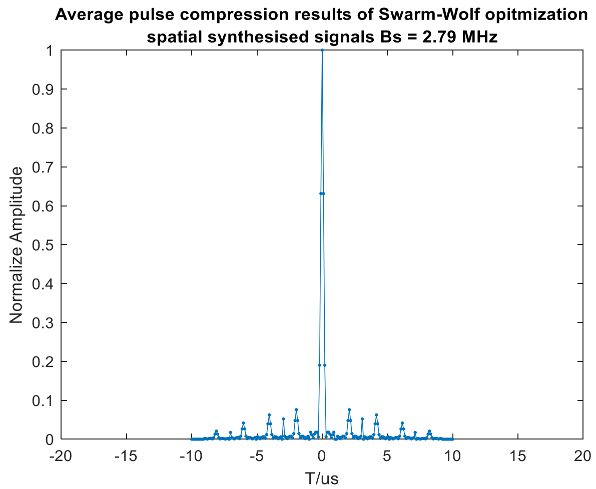

(d)

Fig .6. Average pulse compression analysis Bs = 2.79MHz (a) Conventional spatial synthesized signals (b). Joint optimization based spatial synthesized signals (c). Modified

Similarly, the average cross correlation analysis of the existing and proposed optimization strategies for the two synthesized signals with Bs = 2.16 MHz and 2.79 MHz, respectively, is shown in Fig 7(a) and (b). In this investigation, the developed waveforms' cross correlation levels are examined, and it is found that the property is not improved by the existing approaches when compared to the suggested model. Consequently, the average cross correlation is separately estimated for the traditional (conventional, joint optimization, modified synthesized signals) and proposed PS-GWO techniques with Bs = 2.16MHz and Bs = 2.79MHz in Fig 8 and Fig 9 respectively. Overall, the obtained results indicate that the hybrid PS-GWO technique outperforms the other existing models with improved cross correlation results for both LFM signals.

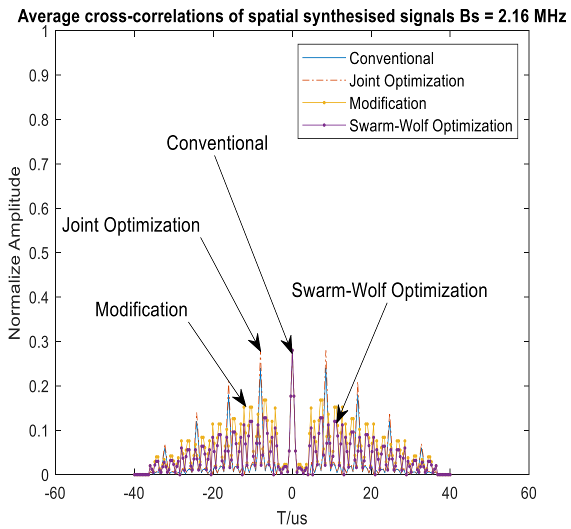

(a)

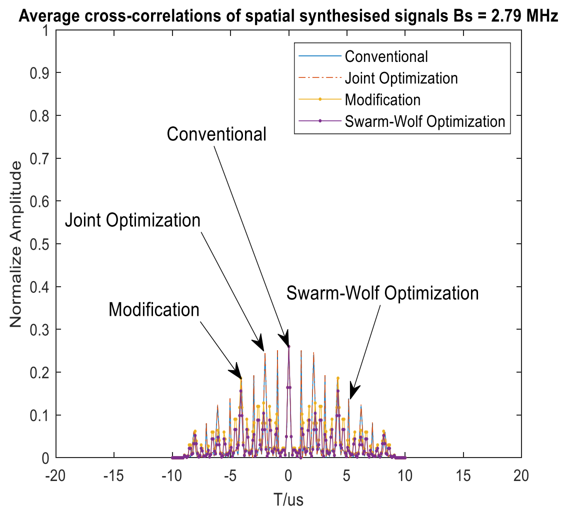

(b)

Fig.7. Average cross correlation analysis (a) Bs = 2.16MHz and (b) = 2.79MHz

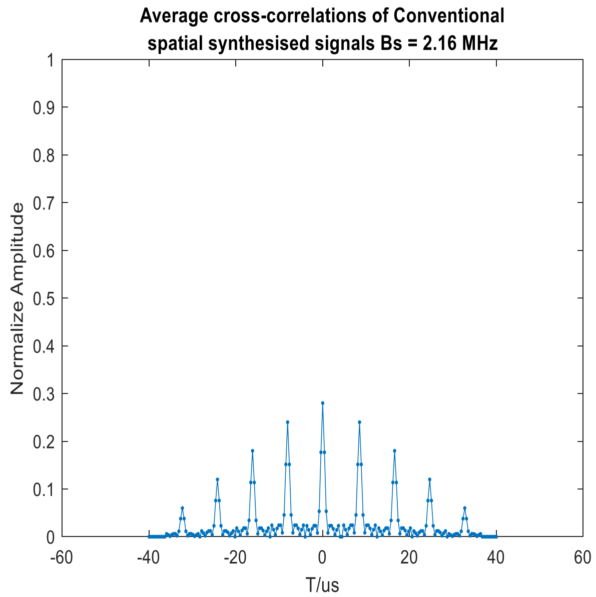

(a)

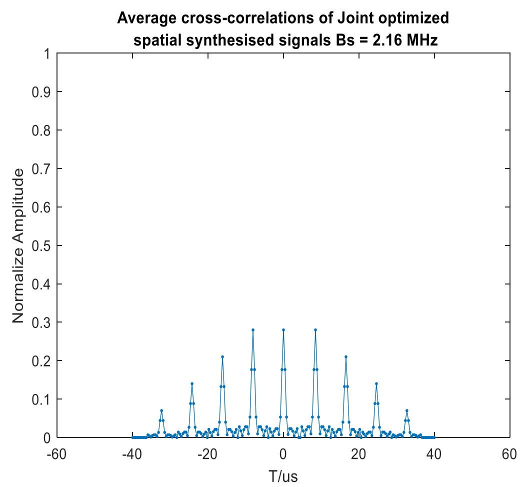

(b)

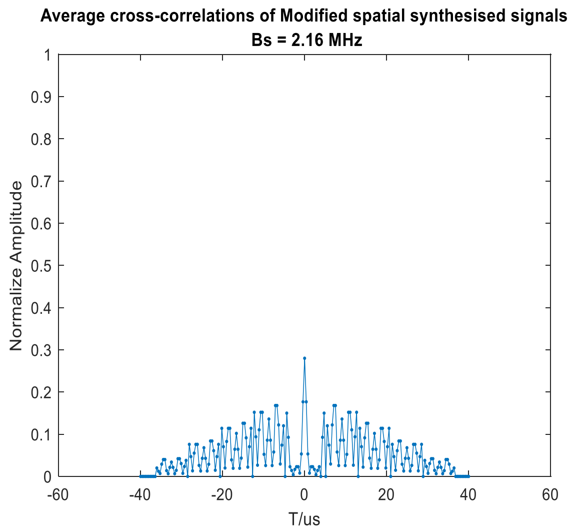

(c)

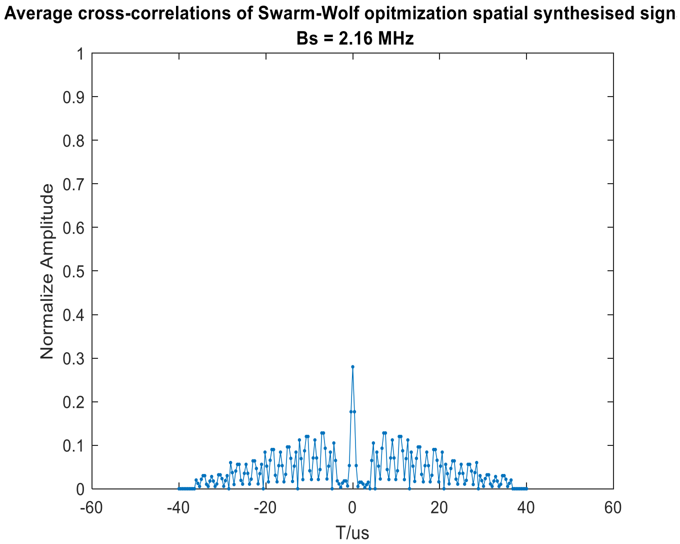

(d)

Fig.8. Average cross correlation results with Bs = 2.16MHz (a) Conventional spatial synthesized signals (b). Joint optimization based spatial synthesized signals (c). Modified spatial synthesized signals, and (d). PS-GWO based spatial synthesized signals

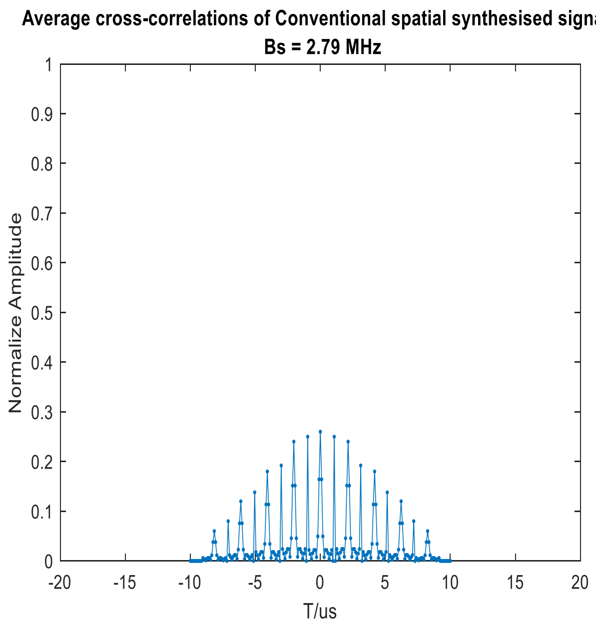

(a)

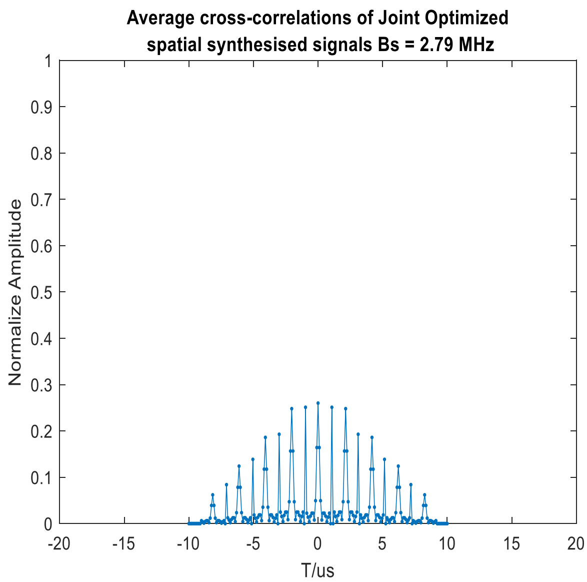

(b)

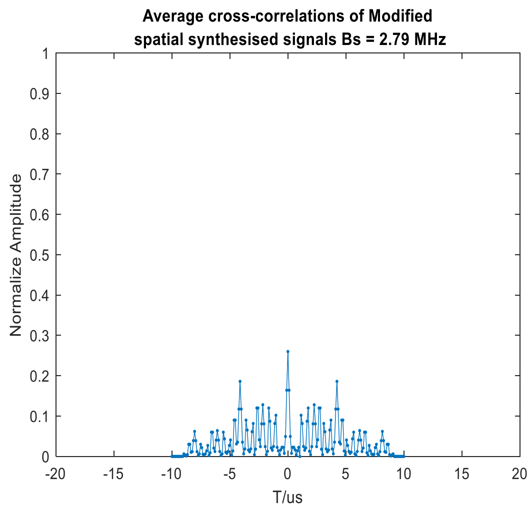

(c)

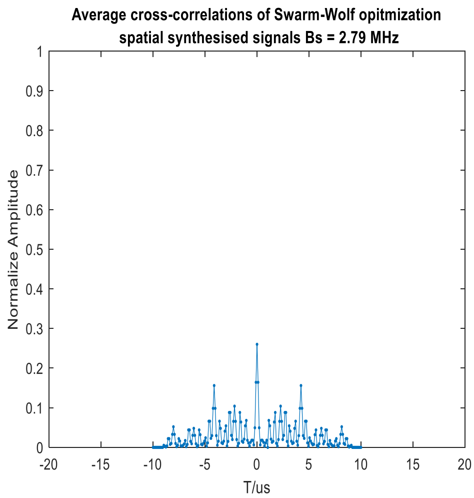

(d)

Fig 9. Average cross correlation results with Bs = 2.79MHz (a) Conventional spatial synthesized signals (b). Joint optimization based spatial synthesized signals (c). Modified spatial synthesized signals, and (d). PS-GWO based spatial synthesized signals

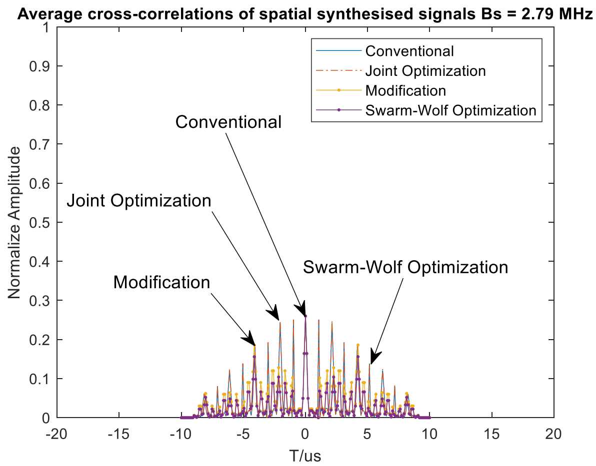

(a)

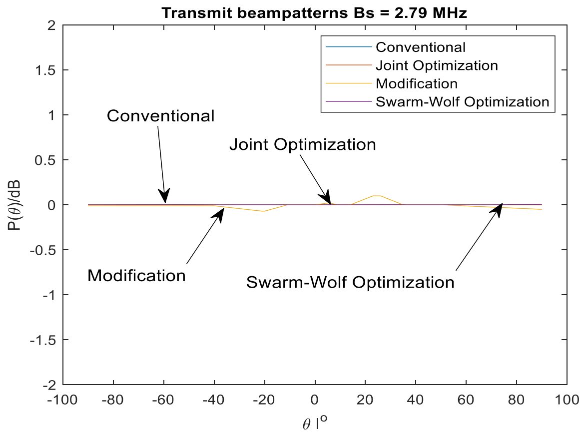

(b)

Fig.10. Transmit beam pattern analysis (a). B_s = 2.16 MHz and (b). B_s = 2.79 MHz

Similar to the autocorrelation analysis, the tweaks made throughout the optimization procedure are what suppress the grating loves. The proposed technique performs better in the cross correlation analysis thanks to the specified waveforms.

As illustrated in Fig. 10, the transmit beam pattern analysis is carried out in a manner similar to that to ascertain the disparity between the joint optimization model and orthogonality. The results show that the transmit beam patterns of the present and suggested models are completely orthogonal. Although it is not satisfied in the modified waveform due to the relaxation of frequency steps, they are roughly orthogonal in the omnidirectional pattern. The pulse compression analysis is displayed in Fig 11 to demonstrate how grating sidelobes operate. According to the analysis, sidelobes can be removed by utilizing the joint optimization model to increase the variety of the frequency step and modulation bandwidth.

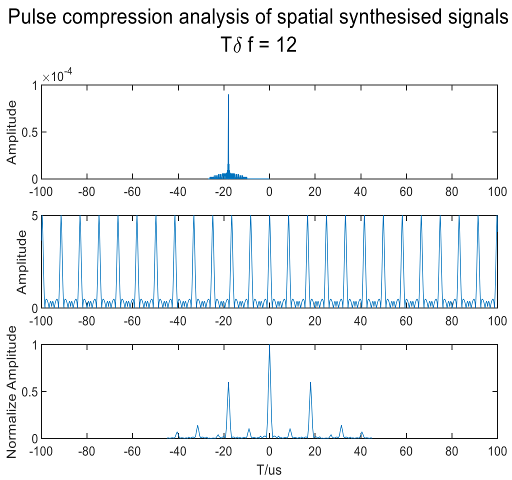

(a)

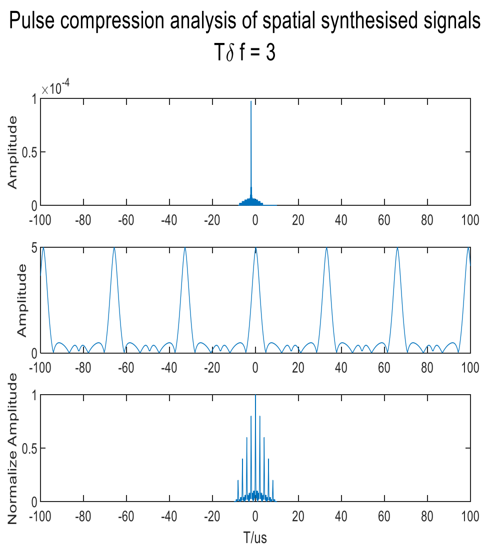

(b)

Fig 11. Pulse compression analysis (a) $T\delta f=2$ and (b) $T\delta f=3$

By using the proposed PS-GWO optimization model, the time duration, bandwidth, arbitrary numbers and frequency steps are efficiently optimized for designing the OFDM-LFM waveforms. The correlation properties considered in this analysis maximum ASP, minimum ASP, and mean CP as shown in Table I, and it also encompasses the parameters of autocorrelation sidelobes, mean cross correlation peals, and mean ASPs. Based on the results, it is determined that the proposed PS-GWO algorithm could effectively reduce the ASPs at varying modulation bandwidths. Hence, the performance of the proposed joint optimization mode is superior than the existing optimization mechanisms. As a result, the suggested joint optimization mode performs better than the current optimization procedures. Table II compares the radiation dull depth of the conventional and proposed optimization techniques. When compared to the other optimization methods [36], it is analyzed that the proposed GW-PSO optimization technique performs the best with a least radiation null notch at 126.9dB.With the help of our developed discrete valued phases, it is possible to create a beam forming network and obtain great performance at a reasonable price. Table III to Table V presents the comparative analysis of the conventional and proposed optimization techniques based on the parameters of Autocorrelation Sidelobe Peak level (ASP), Cross correlation (CP), Auto Correlation Sidelobe Energy (ACSE), and Cross Correlation Energy (CCE). For fair comparison [37], ASP and CP are normalized to the sequence length as shown in Fig 12. Based on the results, it is found that the proposed mechanism is capable of achieving the best ASP (20.5 dB) and ASLE (0.3524) among all, so assures the high range of resolution of the radar communication system.

TABLE I COMPARATIVE ANALYSIS

Method	**Bs, MHz**	**2.72**	**2.44**	**2.16**	**1.81**	**1.46**
Conventional[14]	Max ASP	0.6499	0.4133	0.5208	0.2060	0.3399
	Mean ASP	0.6420	0.4102	0.5208	0.1994	0.3261
	Mean CP	0.5674	0.6405	0.5341	0.6525	0.6367
Joint Optimization[14]	Max ASP	0.2061	0.1745	0.1302	0.1148	0.1384
	Mean ASP	0.2036	0.1724	0.1288	0.1138	0.1373
	Mean CP	0.5539	0.5338	0.5292	0.5312	0.5366
Modified [14]	Max ASP	0.2381	0.1766	0.1376	0.1284	0.1232

	Mean ASP	0.2237	0.1748	0.1354	0.1274	0.1214
	Mean CP	0.4429	0.3639	0.3527	0.3503	0.3829
Optimization Modified (PSO-SQP)	Max ASP	0.1825	0.1602	0.1256	0.1053	0.1126
	Mean ASP	0.1856	0.1525	0.1156	0.1017	0.1021
	Mean CP	0.4251	0.3541	0.3421	0.3385	0.3592
Optimization Modified (PS-GWO-SQP)	Max ASP	0.1451	0.1324	0.0956	0.0853	0.0876
	Mean ASP	0.1473	0.1297	0.0918	0.0805	0.0815
	Mean CP	0.3814	0.3217	0.3136	0.3059	0.3283

TABLE II

Optimized radiation depth analysis

Techniques	*Radiation null depth (dB)*
Enhanced Simulated Annealing (ESA)	-70
Phase Only Variable Metric Method (POVMM)	-105
Jaya Optimization	-124.4
Modified PSO-SQP	-125.8
Proposed GW-PSO	-126.9

TABLE III

AVERAGE ASP ANALYSIS

Optimization techniques	*Average ASP*	
	Normalized value	*In dB*
SA with iterative search	0.1525	-16.33
GA with iterative code selection	0.1471	-16.64
ACO with hamming scan	0.1293	-17.77
Jaya optimization	0.1223	-18.25
Modified (PSO-SQP)	0.1142	-19.4
Proposed GW-PSO	0.1045	-20.5

TABLE IV

Average CP analysis

Optimization techniques	***Average CP***	
	Normalized value	*In dB*
SA with iterative search	0.2798	-10.45
GA with iterative code selection	0.2666	-11.48
ACO with hamming scan	0.2068	-13.68
Jaya optimization	0.2078	-13.64
Modified (PSO-SQP)	0.1989	-14.02
Proposed GW-PSO	0.1824	-15.06

TABLE V

Average ASP and CP analysis

Optimization algorithm	*Average ASLE*	*Average CCE*
SA with iterative search	0.4398	0.4852
GA with iterative code selection	0.4299	0.4754
PSO with Hamming scan	0.4306	0.4681
ACO with hamming scan	0.3993	0.4442
Jaya optimization	0.3828	0.4558
Modified (PSO-SQP)	0.3745	0.4352
Proposed GW-PSO	0.3524	0.4028

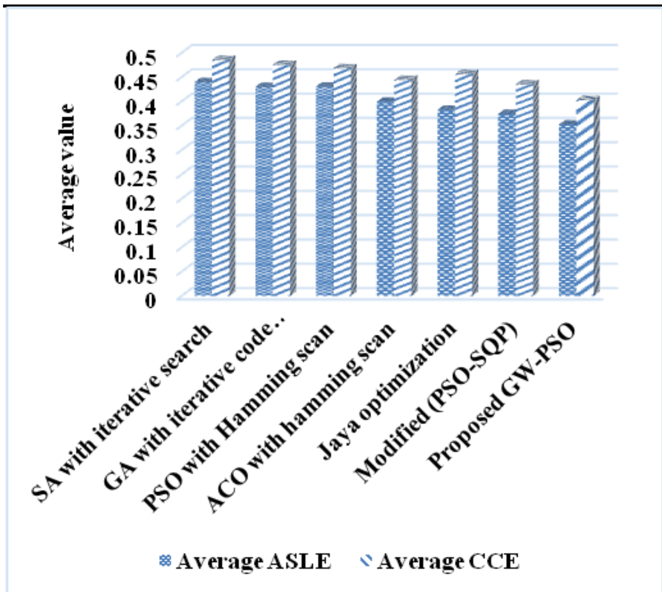

Fig.12. Comparative analysis based on ASLE and CCE

Cross correlation (CP), Auto Correlation Sidelobe Energy (ACSE), and Cross Correlation Energy (CCE). For fair comparison [37], ASP and CP are normalized to the sequence length as shown in Fig 12. Based on the results, it is found that the proposed mechanism is capable of achieving the best ASP (20.5 dB) and ASLE (0.3524) among all, so assures the high range of resolution of the radar communication system.

5. Conclusion

This work introduces a new joint optimization model that combines the PSO and GWO techniques, named as, PS-GWO for constructing the OFDM-LFM waveforms. Here, the optimization approach is mainly used to improve the pulse compression characteristics of generated signals. Conventionally, various existing works are paying close attention to analyze that how to improve the pulse compression feature in MIMO radar communication systems. One of the best methods for choosing frequency codes and phases optimally in order to get rid of grating sidelobes with the perfect orthogonal property is to use joint optimization. Here, increased convergence rate, processing speed, and the ability to find the best solution with the fewest repetitions are the main benefits of adopting the hybrid PS-GWO mechanism. The proposed mechanism's effectiveness is verified through simulation and contrasted with the common joint optimization strategies based on the correlation features. The results show that the proposed PS-GWO optimization mechanism works better than the existing methods with better pulse compression qualities. This study can be expanded in the future by using a new hybrid optimization methodology to boost the functionality of MIMO radar systems.

References

[1] H. Chen, F. Ahmad, S. Vorobyov, and F. Porikli, "Tensor decompositions in wireless communications and MIMO radar," *IEEE Journal of Selected Topics in Signal Processing,* vol. 15, no. 3, pp. 438-453, 2021.

[2] J. Gao, S. Zhu, L. Lan, and X. Li, "Mainlobe Deceptive Jammer Suppression with OFDM-LFM-MIMO Radar based on Blind Source Separation," in *2022 IEEE 12th Sensor Array and Multichannel Signal Processing Workshop (SAM)*, 2022, 20-23 June, Norway, pp. 380-384.

[3] F. Alassery, "Convergence between virtual MIMO and node deployment strategy for high performance multi-hop wireless sensor networks [J]," *IAENG Internaitonal journal of computer science,* vol. 46, no. 2, pp. 349-357, 2019.

[4] T. Liu, J. Sun, Q. Li, Z. Hao, and G. Wang, "Low Correlation Interference OFDM-NLFM Waveform Design for MIMO Radar Based on Alternating Optimization," *Sensors,* vol. 21, no. 22, p. 7704, 2021.

[5] B. Xue, G. Zhang, H. Leung, Q. Dai, and Z. Fang, "An Applied Ambiguity Function Based on Dechirp for MIMO Radar Signal Analysis," *IEEE Geoscience and Remote Sensing Letters,* vol. 19, pp. 1-5, 2022.

[6] Q. Ma, J. Lu, D. Liu, and Y. Kong, "Integrated Waveform Design for Centralized MIMO-OFDM-BPSK-LFM Radar Communication," in *Journal of Physics: Conference Series* 2021, 16-18 April, Tianjin, China, p. 012098.

[7] C. Wen, L. Chen, P. Duan, and X. Cui, "MIMO Radar Imaging With Multiple Probing Pulses for 2D Off-Grid Targets via Variational Sparse Bayesian Learning," *IEEE Access,* vol. 8, pp. 147591-147603, 2020.

[8] Q. Shi, T. Zhang, X. Yu, X. Liu, and I. Lee, "Waveform designs for joint radar-communication systems with OQAM-OFDM," *Signal Processing,* vol. 195, p. 108462, 2022.

[9] P. Mukunthan and P. Dananjayan, "Modified PTS combined with interleaving technique for PAPR reduction in MIMO-OFDM system with different subblocks and subcarriers," *IAENG International Journal of Computer Science,* vol. 39, no.4, pp. 339-348, 2012.

[10] Y. Liu, G. Liao, Z. Yang, and J. Xu, "Joint range and angle estimation for an integrated system combining MIMO radar with OFDM communication," *Multidimensional Systems and Signal Processing,* vol. 30, pp. 661-687, 2019.

[11] W. Haitao, Y. Junpeng, Y. Wenzhen, and B. De, "Adapitive waveform design for distributed OFDM MIMO radar system in multi-target scenario," *Chinese Journal of Aeronautics,* vol. 31, no. 3, pp. 567-574, 2018.

[12] Y. Zhao, X. Lu, J. Yang, W. Su, and H. Gu, "OFDM wavefroms designed with piecewise nonlinear frequency modulation pulse for MIMO radar," *International journal of remote sensing,* vol. 39, no. 23, pp. 8746-8765, 2018.

[13] Y. Cheng, J. Zhang, C. Li, and D. Zhu, "Orthogonal anti-jamming waveform design with extended Doppler tolerance based on the LFM-PC signal," *Digital Signal Processing,* vol. 122, p. 103334, 2022.

[14] C. Sun and M. A. López, "Numerical Simulation of a Multi-Output Radar Orthogonal Waveform Based on a Chaos Optimization Algorithm," *Russian Physics Journal,* vol. 64, pp. 1599-1612, 2022.

[15] H. Zhang, J. Xie, J. Shi, T. Fei, J. Ge, and Z. Zhang, "Joint beam and waveform selection for the MIMO radar target tracking," *Signal Processing,* vol. 156, pp. 31-40, 2019.

[16] Z. Cheng, C. Han, B. Liao, Z. He, and J. Li, "Communication-aware waveform design for MIMO radar with good transmit beampattern," *IEEE Transactions on Signal Processing,* vol. 66, no.21, pp. 5549-5562, 2018.

[17] R. Liu, W. Zhang, X. Yu, Q. Lu, W. Wei, L. Kong*, et al.*, "Transmit-Receive Beamforming for Distributed Phased-MIMO Radar System," *IEEE Transactions on Vehicular Technology,* vol. 71, no. 2, pp. 1439-1453, 2021.

[18] Z. Cheng, B. Liao, and Z. He, "Spectrally compatible waveform design for MIMO radar with transmit beampattern formation," in *2018 IEEE 23rd International Conference on Digital Signal Processing (DSP)* 2018, 19-21 November, Shanghai, China, pp. 1-5.

[19] T. Bai, N. Zheng, and S. Chen, "OFDM MIMO radar waveform design for targets identification," *ETRI Journal,* vol. 40, no.5, pp. 592-603, 2018.

[20] J. Li, G. Liao, Y. Huang, Z. Zhang, and A. Nehorai, "Riemannian geometric optimization methods for joint design of transmit sequence and receive filter on MIMO radar," *IEEE Transactions on Signal Processing,* vol. 68, pp. 5602-5616, 2020.

[21] C. D. Ozkaptan, E. Ekici, C.-H. Wang, and O. Altintas, "Optimal Precoder Design for MIMO-OFDM-based Joint Automotive Radar-Communication Networks," in *2021 19th International Symposium on Modeling and Optimization in Mobile, Ad hoc, and Wireless Networks (WiOpt),* 2021, pp. 1-8.

[22] S. Hong, Y. Dong, R. Xie, Y. Ai, and Y. Wang, "Constrained Transmit Beampattern Design Using a Correlated LFM-PC Waveform Set in MIMO Radar," *Sensors,* vol. 20, no.3, p. 773, 2020.

[23] Z. Xu, C. Fan, and X. Huang, "MIMO radar waveform design for multipath exploitation," *IEEE Transactions on Signal Processing,* vol. 69, pp. 5359-5371, 2021.

[24] H. Zhang, B. Zong, and J. Xie, "Power and bandwidth allocation for multi-target tracking in collocated MIMO radar," *IEEE Transactions on Vehicular Technology,* vol. 69, no.9, pp. 9795-9806, 2020.

[25] L. Min, Y. Han, and Y. Xiang, "A Two-Stage Robust Omega Portfolio Optimization with Cardinality Constraints," *IAENG International Journal of Applied Mathematics,* vol. 53, no.1, 2023.

[26] M. Tang, N. Zhao, X. Ouyang, and F. Zhang, "Event-Triggered Adaptive Prescribed Performance Control of Uncertain MIMO Nonlinear Systems," *IAENG International Journal of Computer Science*, vol. 48, no 4, 2023.

[27] J. Li, Q. Deng, J. Ou, and W. Wang, "Research on Random Redundant Multi-Carrier Phase Code Signal Against Isrj Based on MIMO Radar," *Progress In Electromagnetics Research M,* vol. 110, pp. 97-107, 2022.

[28] L. Huang, X. Deng, L. Zheng, H. Qin, and H. Qiu, "Joint design of colocated MIMO radar constant envelope waveform and receive filter to reduce SINR loss," *Sensors,* vol. 21, no. 11, p. 3887, 2021.

[29] Y. Zhao, M. Ritchie, X. Lu, W. Su, and H. Gu, "Non-continuous piecewise nonlinear frequency modulation pulse with variable sub-pulse duration in a MIMO SAR radar system," *Remote sensing letters,* vol. 11, no.3, pp. 283-292, 2020.

a. Xenaki, Y. Pailhas, and R. Sabatini, "Sparse MIMO synthetic aperture sonar processing with distributed optimization," in *2020 54th Asilomar Conference on Signals, Systems, and Computers*, 2020, 23-25 November, 2020, virtual conference, pp. 82-87.

[30] J. Qian, M. Lops, L. Zheng, X. Wang, and Z. He, "Joint system design for coexistence of MIMO radar and MIMO communication," *IEEE Transactions on Signal Processing*, vol. 66, no.13, pp. 3504-3519, 2018.

[31] X. Wang, A. Hassanien, and M. G. Amin, "Dual-function MIMO radar communications system design via sparse array optimization," *IEEE Transactions on Aerospace and Electronic Systems*, vol. 55, no. 3, pp. 1213-1226, 2018.

[32] M. Rihan and L. Huang, "Optimum co-design of spectrum sharing between MIMO radar and MIMO communication systems: An interference alignment approach," *IEEE Transactions on Vehicular Technology*, vol. 67, no. 12, pp. 11667-11680, 2018.

[33] Q. Shi, X. Li, T. Zhang, G. Cui, and L. Kong, "OQAM-OFDM Radar approximated IRCI-free pulse compression," *IEEE Transactions on Vehicular Technology,* vol. 69, no.9, pp. 10009-10018, 2020.

[34] B. E. Martinez, M. A. Castro-Coria, J. Cerda, and A. Avalos, "An Efficient Method to Obtain Bifurcation Diagrams based on PSO Algorithms," in *Lecture Notes in Engineering and Computer Science: Proceedings of The World Congress on Engineering and Computer Science* 2018, 23-25 October, 2018, San francisco, USA, pp. 23-25.

[35] P. Bhamre and S. Gupta, "Constrained waveform designing for MIMO radar using Jaya optimization," *Wireless Personal Communications*, vol. 111, pp. 331-342, 2020.

[36] W. Wongsinlatam and S. Buchitchon, "Criminal cases forecasting model using a new intelligent hybrid artificial neural network with cuckoo search algorithm," *IAENG International Journal of Computer Science*, vol. 47, no.3, pp. 481-490, 2020